Appl Phys B (2011) 102: 769–774
DOI 10.1007/s00340-010-4201-9

Applied Physics B
Lasers and Optics

High-fidelity front-end for high-power, high temporal quality few-cycle lasers

A. Jullien · X. Chen · A. Ricci · J.-P. Rousseau · R. Lopez-Martens · L.P. Ramirez · D. Papadopoulos · A. Pellegrina · F. Druon · P. Georges

Received: 4 May 2010 / Revised version: 25 June 2010 / Published online: 15 September 2010

Abstract A 80 μJ, 6 fs, CEP-stable high-contrast injector is demonstrated. The device relies on standard pulse post-compression in hollow-core fiber followed by a temporal filter based on cross-polarized wave generation. Pulses with a Gaussian spectrum over 350 nm, centered at 750 nm, are generated. Temporal measurements show that the contrast of the few-cycle pulses is enhanced on a femtosecond and picosecond time scale. The carrier-envelope phase stability is preserved (0.3 rad RMS). These performances make the system an ideal seed laser for high-power, high-contrast OPCPA systems.

Multi-terawatt few-cycle light pulses offer attractive prospects in high-energy density physics [1]. Recently, the acceleration of bright and quasi mono-energetic bunches of electrons by few-cycle, multi-millijoule laser pulses, has been predicted and experimentally realized [2, 3]. Significant developments are expected for the generation of energetic attosecond pulses, via the interaction of intense pulses with solid density plasmas [4–7]. This technique should lead to orders of magnitude gain in the attosecond pulse energy. Furthermore, multi-terawatt few-cycle chains are developed as front-end injectors of future ultrashort petawatt-scale peak power lasers [8, 9].

Optical parametric chirped pulse amplification (OPCPA) provides a larger amplification spectral bandwidth than conventional femtosecond Ti:Sa lasers and therefore constitutes the main technique for the production of multi-millijoule sub-10 fs pulses [10–12]. As the temporal contrast of the laser pulses is a major requirement for laser-solid targets interactions [6, 13, 14], sources of low energy (∼100 μJ), high-temporal quality few-cycle pulses are needed as injectors for high-power OPCPA systems to enhance the final contrast [15]. Ideally, such ultrashort seed pulses should feature a very low level of ASE (amplified spontaneous emission, incoherent contrast) and a high spectral quality in order to minimize the intensity of the coherent pedestal and satellite pulses (coherent contrast). The preservation of the carrier-envelope phase (CEP) stability is also required. Currently, high-power OPCPA systems are seeded with a CEP-stable Ti:Sa lasers followed by post-compression in a hollow-core fiber (HCF). Millijoule-level Ti:Sa lasers typically exhibit an ASE background relative to the main peak between 10^{-6} and 10^{-8}. The subsequent spectral broadening through the HCF leads to strong modulations and sharp features of the spectral amplitude and distorted spectral phase [16, 17]. The resulting few-cycle pulses present a poor temporal quality on the few-ps to few-fs range [18, 19]. As a consequence, the temporal quality of current OPCPA systems has still to be improved [6, 12].

A. Jullien (✉) · X. Chen · A. Ricci · J.-P. Rousseau · R. Lopez-Martens
Laboratoire d'Optique Appliquée, ENSTA ParisTech, Ecole Polytechnique, CNRS, UMR 7639, 91761 Palaiseau Cedex, France
e-mail: Aurelie.Jullien@ensta-paristech.fr

X. Chen · D. Papadopoulos · A. Pellegrina
Institut de la Lumière Extrême CNRS, Ecole Polytechnique, ENSTA ParisTech, Institut d'Optique, Univ Paris-Sud, Palaiseau Cedex, France

A. Ricci
Thales Optronique SA, Laser Solutions Unit, 78995 Elancourt, France

L.P. Ramirez · D. Papadopoulos · A. Pellegrina · F. Druon · P. Georges
Laboratoire Charles Fabry de l'Institut d'Optique, CNRS, Univ Paris-Sud, 91127 Palaiseau, France

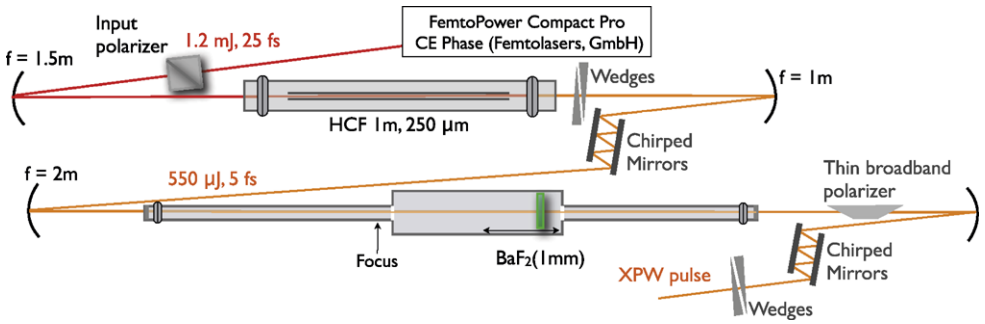

Fig. 1 Experimental setup

Cross-polarized wave (XPW) generation in $\chi^{(3)}$-anisotropic crystals (typically BaF_2) is a well-known technique leading to significant improvement of the contrast of femtosecond pulses and to remarkable spectral smoothing and broadening [20–22]. Furthermore, it has been recently shown that XPW generation preserves the CEP [23]. In a previous publication, we demonstrated the possibility of extending XPW filtering to the few-cycle regime [24]. As a proof of principle, 8 fs, 150 µJ pulses with a modulated spectrum were seeded to a single-crystal XPW filter, with an overall energy efficiency of 10%. It was experimentally and theoretically found that the optimization of the pulse compression enabled preserving the input spectral bandwidth while the XPW spectrum exhibited a smooth near-Gaussian shape.

In this paper, we characterize an ideal front-end for high-power contrasted lasers based on standard hollow-core fiber post-compression combined with XPW technique. We scale the few-cycle XPW filter to shorter (5 fs) and higher-energy (550 µJ) pulses. We demonstrate that fine dispersion control provides high transmission (15%) and a quasi-Gaussian XPW spectrum over 350 nm. The resulting injector generates on a day-to-day basis 80 µJ pulses with a duration of 5.9 fs. Temporal characterization of the generated pulses shows significantly enhanced coherent contrast, which is a critical feature of few-cycle pulses. Furthermore, we provide an estimation of the expected improvement of incoherent contrast. We finally demonstrate that the front-end is CEP-stable with a RMS error signal of 0.3 rad RMS.

The experimental setup (Fig. 1) features a commercial 1 kHz CEP-stabilized laser (FemtoPower Compact Pro CE-Phase, Femtolasers GmbH). The oscillator pulses are CEP locked via pump-laser amplitude modulation, stretched to ∼10 ps through a SF57 glass block unit and amplified in a ten-pass amplifier. The pulses are then compressed in a compact transmission grating compressor preserving the CEP stability [25, 26]. After compensation of the slow drift via feedback on the stretcher, the typical RMS CEP stability value is 0.2 rad. The 25 fs pulses, with an energy set to 1.2 mJ, are focused into a hollow-core fiber (HCF, 1 m length, 250 µm diameter) filled with neon (about 1 bar) [27]. The setup dispersion is then over-compensated with a set of broadband chirped mirrors (∼–580 fs^2) which was found

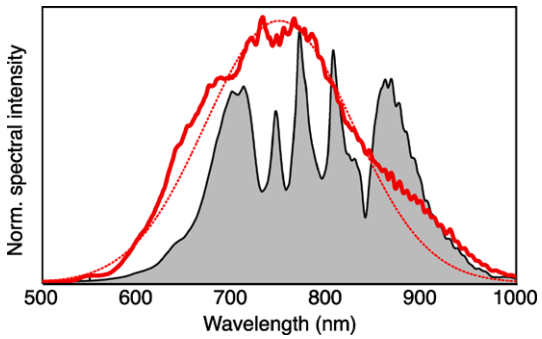

Fig. 2 Experimental spectra of the pulses out of the HCF (*grey area*) and after XPW (*red*). The XPW spectrum is measured when the dispersion compensation of the input pulse yields the optimum spectral shape and highest efficiency (15%). The *dashed red line* is a Gaussian fit of the XPW spectral energy distribution

to minimize high-order spectral phase (Femtolasers GmbH and Layertec GmbH). A pair of fused-silica wedges is used to fine tune pulse compression. The compressed 550 µJ, 5 fs pulses are then sent into in the XPW filter. The beam is focused by a $f = 2$ m mirror into a small vacuum chamber with coated 500 µm fused-silica windows. The nonlinear crystal is 1 mm thick (BaF_2, [011] crystallographic orientation) and placed after the focus (50 cm) to reach the adequate peak intensity for XPW generation (the beam diameter is 2 mm). Thanks to the excellent spatial quality of the beam after propagation through the HCF, the spatial profile stays smooth and un-modulated after the focus. The XPW signal is then discriminated by a broadband thin film polarizer (Femtolasers GmbH). This polarizer induces low dispersion and has a good transmission over a broad spectral bandwidth but its polarizing efficiency is limited, which will directly affect the overall contrast enhancement [20]. With an input Glan polarizer placed before the HCF, the global extinction ratio of the setup is $10^2 : 1$, limited by the output polarizer. This value could be improved by using an output Glan polarizer if the temporal compression of the XPW pulse is not necessary (for example before seeding OPCPA stages). To perform temporal characterization, a second set of chirped mirror (Femtolasers, ∼–500 fs^2) and wedges compensates the dispersion introduced by the BaF_2 crystal, the output window, the polarizer and propagation in air.

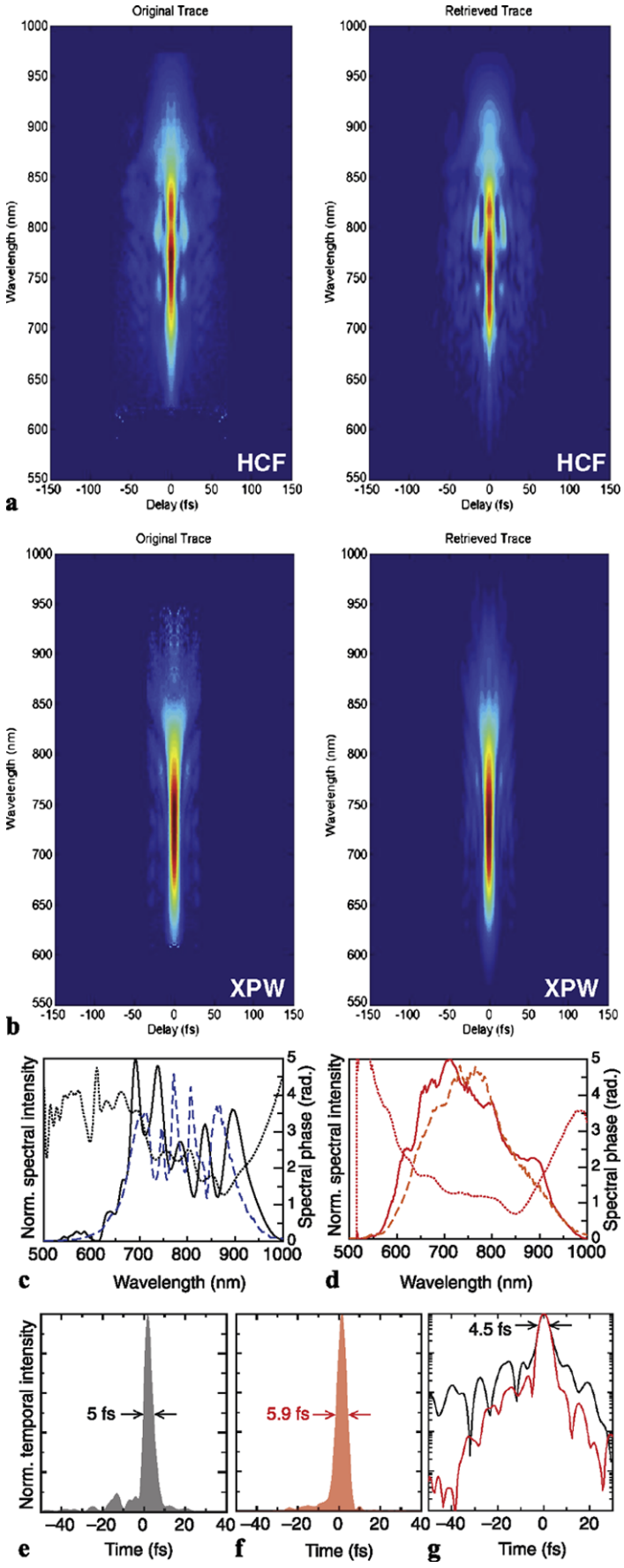

Fig. 3 Original (*left*) and retrieved (*right*) SHG-FROG traces measured after the HCF (**a**) and after XPW (**b**), with a respective retrieval error of 0.5% and 0.3% (grid size 256 × 256). Measured (*dashed lines*) and retrieved (*solid lines*) spectral amplitude and phase (*dotted lines*) after the HCF (**c**) and after XPW (**d**). Temporal profile of the few-cycle pulses after the HCF (**e**) and after XPW (**f**). (**g**) Temporal profiles (log scale) of the few-cycle pulses after calculated propagation in fused-silica glass of the pulses retrieved by the FROG measurement. *Black*: after the HCF (+50 μm). *Red*: after XPW (−200 μm)

According to our previous investigations, an accurate tuning of the input pulse dispersion (wedges) optimizes the XPW process in terms of efficiency and spectral cleaning. An analysis of the dynamics of the XPW generation process as a function of the input chirp and the effects of the dispersion of the nonlinear medium is detailed in [24]. The 1 mm nonlinear crystal introduces some temporal broadening of the input few-cycle pulse and the resulting chirped temporal structure of the propagating pulse in some parts of the BaF_2 limits the XPW spectral bandwidth. In particular, no spectral broadening is observed, unlike for longer input pulses. It was found that weak negative residual input chirp, leading to temporal compression of the fundamental pulse roughly halfway through the nonlinear crystal, enables preserving the input spectral bandwidth. In that case, most of the conversion occurs on an almost compressed pulse, optimizing the efficiency and output spectrum. In the current experiment, the precise window for optimum compression (± 4 fs^2) is experimentally determined by the XPW spectral behavior: the spectral bandwidth is preserved during the nonlinear process and the output shape is quasi-Gaussian over 350 nm (Fig. 2). The cleaning of the input spectral energy distribution is remarkable. Outside this compression window, the XPW spectrum is either narrower than the fundamental (negative residual chirp), or square-shaped (positive residual chirp). The optimum spectral shape corresponds to the maximum XPW efficiency (15%, XPW pulse energy: 80 μJ). The transmission decreases rapidly outside the optimum compression configuration. The final energy level is comparable with the reported energy of other OPCPA injectors [8, 12] and enables temporal characterization of the pulses after the XPW cleaning process.

Temporal characterization of the pulses before and after XPW confirms that the excellent spectral properties of the XPW pulse are the consequence of the temporal quality enhancement occurring during the process. Figure 3 presents the $\chi^{(2)}$-based frequency-resolved optical gating (SHG-FROG) measurements [28]. Comparison between the FROG traces underscores the reduction by the XPW process of the temporal side lobes and sharp features typical of few-cycle pulses (Fig. 3(a), (b)). The spectro-temporal energy distribution is more balanced and homogeneous. To confirm the accuracy of the FROG reconstruction, the retrieved spectrum is shown together with the measured spectrum (Fig. 3(c), (d)). The temporal intensity profiles of both pulses appear in Fig. 3(e), (f). The coherent background is clearly attenuated on a femtosecond time scale after XPW. In this case, the main peak (Gaussian pulse with the same duration) contains 90% of the pulse energy, compared with only 75% after the HCF. This feature represents a significant improvement of the usual characteristics of few-cycle pulses, which can be further improved by adequate high-order spectral phase compensation. Although the whole spectral bandwidth of the pulse is preserved during the process, the measured duration of the XPW pulse is 5.9 fs, a little longer than the initial one (5 fs). Indeed, the FROG data analysis requires to run a non real-time algorithm, thus precluding a precise duration optimization during the experiment. Calculated propagation in fused-silica glass of the measured pulses indicates the shortest accessible duration: 4.5 fs in both cases (after HCF and XPW) (Fig. 3(g)). The resulting plot emphasizes again the improved temporal quality of the XPW pulse on a femtosecond time scale.

Besides, the XPW process is known to enable enhancement of the temporal contrast on a picosecond time scale, limited by the polarization extinction ratio. Consequently, we expect the contrast to be improved by 2 orders of magnitude after XPW. However, the measurement of the absolute contrast ratio with a high-dynamic third-order correlator remains technically challenging in the proposed experiment, because of the weak pulse energy and the involved spectral bandwidth. The optical components in the employed standard correlator (SEQUOIA type) introduces important spectral clipping. This spectral clipping, together with the dispersion introduced by various optical elements, unavoidably induces a reduced pulse contrast measurement [11]. This effect is shown in the inset of Fig. 4, representing the correlation curves of the laser pulse and measured after pulse compression in the HCF. The temporal features on the leading edge of both pulses are similar, except a degradation of the contrast ratio of the 5 fs pulse. This can be attributed to the peak power degradation due to spectral clipping in

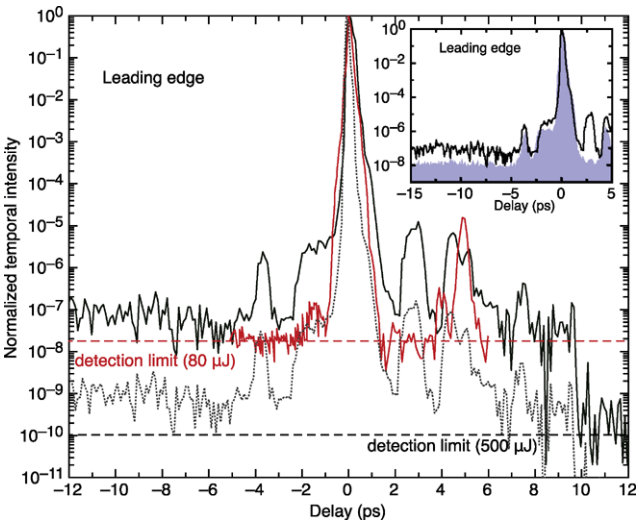

Fig. 4 Temporal contrast of the few-cycle pulses before (*black*) and after (*red*) XPW. The *dashed lines* indicate the dynamic range of the measurement in both cases (10^{-10} after the HCF and 10^{-8} after XPW). The *dotted curve* is the calculated contrast after XPW. The *inset* shows the measured contrast of the laser pulse (*grey area*) and the pulse after HCF (*black line*). The temporal resolution of the correlator does not allow to make statements about the time structure of the main peak

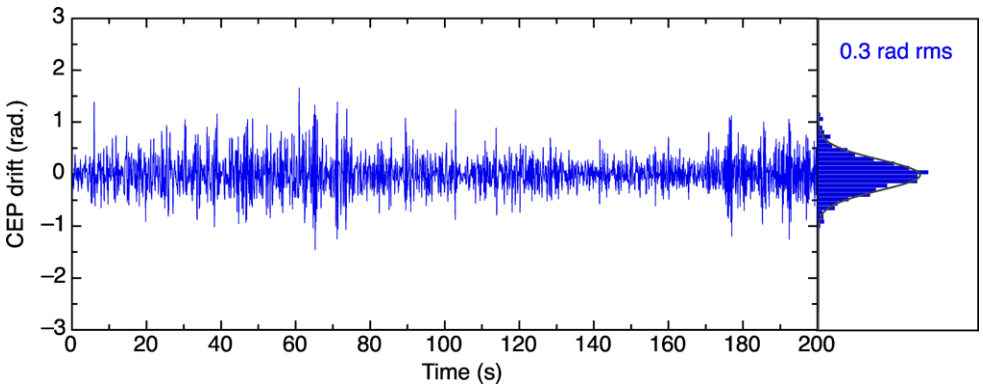

Fig. 5 Measured stabilized CEP drift of the XPW pulse with feedback control

the correlator. Anyway, this does not prevent to perform a relative measurement of the contrast enhancement after XPW in the few-cycle regime. The results shown in Fig. 4 indicate a 2 orders of magnitude contrast improvement by the diminution of the intensity of the parasitic features at $t = -5$ ps and $t = -1$ ps. The ASE background value cannot be measured because of the dynamic range limitation of the apparatus (8 orders of magnitude for a seed energy of 80 μJ). Anyway, considering previous work on XPW, we expect a similar contrast improvement (10^{-2}), as suggested by the calculated XPW contrast ratio (Fig. 4). This calculation is performed via the model proposed in [29], including the experimental parameters (extinction ratio: 10^{-2}; overall efficiency: 15%). A good agreement with the experimental measurement above the detection limit is obtained.

Finally, we demonstrate that the proposed setup preserves the relative CEP stability. A part of the compressed XPW pulse is sent into a collinear f-to-2f interferometer. The pulse is focused into a 0.5 mm thick BBO crystal preceded by a sapphire plate to slightly enhance the spectral bandwidth. The interference fringes are acquired by a spectrometer (integration time: 1 ms) and analyzed by the APS 800 software (Menlo Systems, cycle loop time: 100 ms). The signal is then fed back to the laser stretcher to compensate for the phase slow drift. The resulting CEP drift measured over 200 s is shown in Fig. 5. The CEP stability is preserved after quite a long propagation distance and two successive nonlinear stages. This feature is the ultimate proof of the high fidelity and reliability of the injector. The CEP stability (0.3 rad RMS) could be improved by simple covering of the whole experimental setup to avoid air fluctuations.

To conclude, we have demonstrated the generation of high temporal quality, CEP-stable, 5 fs, 80 μJ pulses. The technique relies on spectro-temporal cleaning of high-energy few-cycle pulses by an optimized vacuum XPW filter. For the first time, the enhancement of the temporal quality of the 5 fs pulses by the XPW process is demonstrated by FROG measurement. We believe that the proposed system is an ideal front-end for high-energy, high-contrast few-cycle lasers.

Acknowledgements The authors gratefully acknowledge P. Monot for the high-dynamical contrast measurements. This work has been funded by the Agence Nationale pour la Recherche, through program ANR-09-JCJC-0063 (UBICUIL), the ILE 07-CPER 017-01 contract, the Canadian National Research Council–Centre National de la Recherche Scientifique (CNRS) 2007 program, and the National Natural science Foundation of China (60908008).

References

1. F. Krausz, M. Ivanov, Rev. Mod. Phys. **81**, 163 (2009)
2. M. Geissler, J. Schreiber, J.M. ter Vehn, New J. Phys. **8**, 186 (2006)
3. K. Schmid, L. Veisz, F. Tavella, S. Benavides, R. Tautz, D. Herrmann, A. Buck, B. Hidding, A. Marcinkevicius, U. Schramm, M. Geissler, J. Meyer-ter Vehn, D. Habs, F. Krausz, Phys. Rev. Lett. **102**, 124 (2009)
4. C. Thaury, H. George, F. Quere, R. Loch, J.P. Geindre, P. Monot, P. Martin, Nat. Phys. **4**, 631 (2008)
5. Y. Nomura, R. Horlein, P. Tzallas, B. Dromey, S. Rykovanov, Z. Major, J. Osterhoff, S. Karsch, L. Veisz, M. Zepf, D. Charalambidis, F. Krausz, G.D. Tsakiris, Nat. Phys. **5**, 124 (2009)
6. R. Horlein, Ph.D. thesis, Ludwig-Maximilians-Universitat (2008)
7. N.M. Naumova, C.P. Hauri, J.A. Nees, I.V. Sokolov, R. Lopez-Martens, G.A. Mourou, New J. Phys. **10**, 025 (2008)
8. I. Ahmad, S. Trushin, Z. Major, C. Wandt, S. Klingebiel, T.-J. Wang, V. Pervak, A. Popp, M. Siebold, F. Krausz, S. Karsch, Appl. Phys. B **97**, 529 (2009)
9. J.P. Chambaret, F. Canova, R. Lopez-Martens, G. Cheriaux, G. Mourou, A. Cotel, C.L. Blanc, F. Druon, P. Georges, N. Forget, F. Ple, M. Pittman, in *Lasers and Electro-Optics, CLEO* (2007)
10. F. Tavella, Y. Nomura, L. Veisz, V. Pervak, A. Marcinkevičius, F. Krausz, Opt. Lett. **32**, 2227 (2007)
11. S. Witte, R.T. Zinkstok, A.L. Wolf, W. Hogervorst, W. Ubachs, K.S.E. Eikema, Opt. Express **14**, 8168 (2006)
12. D. Herrmann, L. Veisz, R. Tautz, F. Tavella, K. Schmid, V. Pervak, F. Krausz, Opt. Lett. **34**, 2459 (2009)
13. A.S. Pirozhkov, S.V. Bulanov, A. Sagisaka, H. Daido, T.Z. Esirkepov, M. Mori, Phys. Plasmas **13**, 013107 (2006)
14. C. Thaury, F. Quéré, J.P. Geindre, A. Levy, T. Ceccotti, P. Monot, M. Bougeard, F. Réau, P. D'Oliveira, P. Audebert, R. Marjoribanks, P. Martin, Nat. Phys. **3**, 424 (2007)
15. F. Tavella, A. Marcinkevičius, F. Krausz, New J. Phys. **8**, 219 (2006)
16. A.J. Verhoef, J.S.K. Schmid, Y. Nnomura, G. Tempea, L. Veisz, F. Krausz, Appl. Phys. B **82**, 513 (2006)
17. S. Bohman, A. Suda, M. Kaku, M. Nurhuda, T. Kanai, S. Yamaguchi, K. Midorikawa, Opt. Express **16**, 10684 (2008)

18. C. Dorrer, J. Bromage, Opt. Express **16**, 3058 (2008)
19. K. Osvay, M. Csatári, I.N. Ross, A. Persson, C.G. Wahlström, Lasers Part. Beams **23**, 327 (2005)
20. A. Jullien, O. Albert, F. Burgy, G. Hamoniaux, J.-P. Rousseau, J.-P. Chambaret, F. Augé-Rochereau, G. Chériaux, J. Etchepare, N. Minkovski, S.M. Saltiel, Opt. Lett. **30**, 920 (2005)
21. A. Jullien, J.-P. Rousseau, B. Mercier, L. Antonucci, O. Albert, G. Chériaux, S. Kourtev, N. Minkovski, S.M. Saltiel, Opt. Lett. **33**, 2353 (2008)
22. V. Chvykov, P. Rousseau, S. Reed, G. Kalinchenko, V. Yanovski, Opt. Lett. **31**, 1456 (2006)
23. K. Osvay, L. Canova, C. Durfee, A.P. Kovács, A. Börzsönyi, O. Albert, R.L. Martens, Opt. Express **17**, 22358 (2009)
24. A. Jullien, C.G. Durfee, A. Trisorio, L. Canova, J.P. Rousseau, B. Mercier, L. Antonucci, G. Cheriaux, O. Albert, R. Lopez-Martens, Appl. Phys. B **96**, 293 (2009)
25. L. Canova, X. Chen, A. Trisorio, A. Jullien, A. Assion, G. Tempea, N. Forget, T. Oksenhendler, R. Lopez-Martens, Opt. Lett. **34**, 1333 (2009)
26. X. Chen, L. Canova, A. Malvache, A. Jullien, R. Lopez-Martens, C. Durfee, D. Papadopoulos, F. Druon, Appl. Phys. B **99**, 149 (2010)
27. M. Nisoli, S.D. Silvestri, O. Svelto, R. Szipöcs, K. Ferencz, C. Spielmann, S. Sartania, F. Krausz, Opt. Lett. **22**, 522 (1997)
28. S. Akturk, C. D'Amico, A. Mysyrowicz, J. Opt. Soc. Am. B **25**, A63 (2008)
29. A. Jullien, O. Albert, G. Chériaux, J. Etchepare, S. Kourtev, N. Minkovski, S.M. Saltiel, Appl. Phys. B **84**, 409 (2006)